Non-equilibrium dynamics of interacting Fermi systems in quench experiments

Mehrtash Babadi[1], David Pekker[1], Rajdeep Sensarma[1], Antoine Georges[2,3], Eugene Demler[1]

[1] *Physics Department, Harvard University, Cambridge, Massachusetts 02138, USA*
[2] *Centre de Physique Theorique, Ecole Polytechnique, CNRS, 91128 Palaiseau Cedex France*
[3] *College de France, 11 place Marcelin Berthelot, 75231 Paris Cedex 05, France*

We describe the dynamics of two component non-interacting ultracold Fermions which are initially in thermal equilibrium and undergo a rapid quench to either the repulsive or attractive side of a Feshbach resonance. The short time dynamics is dominated by the exponentially growing collective modes. We study the Stoner instability and formation of ferromagnetic textures on the repulsive side, and the pairing instability towards BCS or FFLO-like states (determined by the population imbalance) on the attractive side. In each case, we evaluate the growth rate of unstable modes and predict the typical lengthscale of textures to be formed.

Non-equilibrium dynamics of strongly interacting quantum many body systems is a subject of great interest with diverse applications in different fields, from condensed matter physics to high energy physics to cosmology. However, compared to equilibrium physics, it lacks deeper understanding from both theoretical and experimental standpoints. Recent developments with ultracold atoms [1] have opened a new window to study strongly interacting model Hamiltonians. Although the focus has been mostly on studying the equilibrium phases of these models, these systems also present a unique opportunity to probe the intrinsic non-equilibrium dynamics in the strongly correlated regime [2]. The low energy scales in the system (typically $\sim$ kHz) and an almost ideal insulation from the environment results in comparatively larger timescales of dynamics than in the corresponding condensed matter systems and therefore, make it easier to follow the intrinsic quantum evolution of the system in real time [3].

The inherent tunability of interactions in these systems allows us to study the dynamics of the system after a quench (rapid change) of the Hamiltonian parameter. In fact, quench dynamics has already been studied in cold atom experiments that probe dynamics and pattern formation in spinor BEC [4], collapse and revival in optical latices [5], and "Bose novae" in BEC's with attractive interactions [6]. Our primary motivation for this study comes from recent experiments on cold two-component Fermions in which interactions are tuned to the strong repulsive regime during the course of the experiment [7]. It was found that for sufficiently strong coupling, the atom loss rate, the size of the atomic cloud and the distribution of the kinetic energy of the atoms show signatures of a transition to a ferromagnetic state. Originally, these experiments were interpreted as probing the equilibrium Stoner transition [8]. On the other hand, the time scales for tuning the interactions between small and large values were limited by the formation of molecules on the BEC side of the Feshbach resonance. In this paper we show that the finite experimental time scales are such that we can also analyze some aspects of the experiments from the point of view of quench dynamics.

In this letter, we focus on the initial dynamics of the collective modes in Fermionic systems following a rapid quench. Within linear response theory, we find that for quenches across a critical interaction strength U_c, some collective modes become dynamically unstable. We denote the growth rate corresponding to an unstable mode with wavevector q by Δ_q. In general, the lengthscale of the textures formed in the quench is bounded by the smallest unstable wavelength q_{cut}^{-1}. Furthermore, if the most unstable mode (i.e. for which Δ_q assumes its maximum) has a finite momentum, q_{max}, then the order parameter will have large spatial modulations at the corresponding wavelength q_{max}^{-1}. We study two typical cases of dynamical instability in Fermi systems starting with a non-interacting gas: (i) quench to the regime of strong repulsive interactions which leads to the Stoner instability and ferromagnetic textures; (ii) quench to the regime of weak attractive interactions and the BCS pairing instability. The order parameter in the former case (magnetization) is conserved, while in the latter case (wavefunction of the coherent pairs), it is not conserved.

Our main results are: (a) for the Stoner instability in 3D, the wave-vector of the most unstable mode scales as $q_{max} \sim u^{1/2}$ while its growth rate $\Delta_{max} \sim u^{3/2}$, where $u = U_f/U_c - 1$ and U_f the final coupling after the quench. (b) In 2D, at $T = 0$, the most unstable mode has growth rate $\sim u$ and occurs at $\sqrt{2}k_F$, where k_F is the Fermi wave-vector of the gas. However, the system is very sensitive to thermal fluctuations and at finite temperatures, q_{max} scales with $u^{1/2}T^{1/2}\exp(\epsilon_F/2T)$ while the growth rate $\sim u\, q_{max}$. This scaling reverts back to its $T = 0$ form once $q_{max} \sim \sqrt{2}k_F$. (c) In the BCS case (in 3D), we find that for small initial spin imbalances, the fastest growing instability is towards formation of coherent Cooper pairs with center of mass momentum $\mathbf{q} = 0$. Beyond a critical polarization, the fastest growing modes correspond to pairings at a finite wavevector, i.e. towards FFLO-like states [9]. Beyond a 2nd critical polarization, all modes become stable. We note that the change in the character of dynamics does not necessarily correspond to crossing a thermodynamic phase transition during the quench; e.g. although there is no ferromagnetic transition in 2D at finite temperatures, quench dynamics still involves unstable modes which exhibit exponential growth.

Formalism– We consider a system of interacting Fermions described by the Hamiltonian:

$$H = \sum_{\mathbf{k},\sigma} \xi_{\mathbf{k}\sigma} c_{\mathbf{k}\sigma}^\dagger c_{\mathbf{k}\sigma} + U(t) \int d^d\mathbf{r}\, c_{\mathbf{r}\uparrow}^\dagger c_{\mathbf{r}\downarrow}^\dagger c_{\mathbf{r}\downarrow} c_{\mathbf{r}\uparrow}, \quad (1)$$
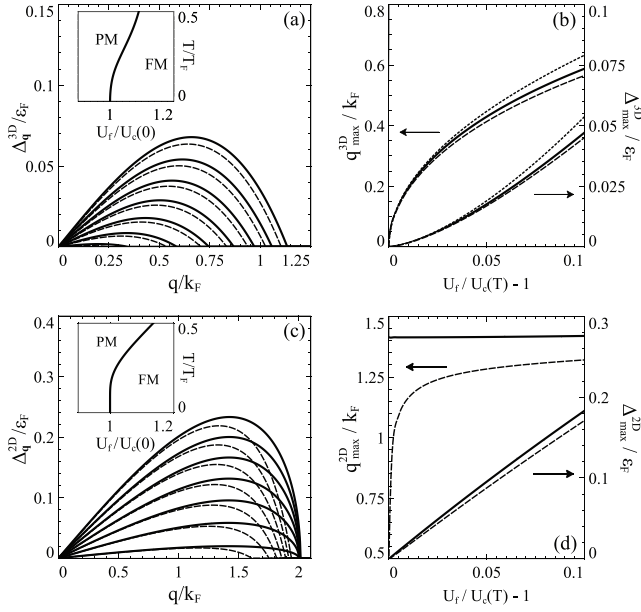
FIG. 1: Properties of growing collective modes in the Stoner instability in 3D (top row) and 2D (bottom row). (a) and (c): Growth rate Δ_q as a function of wavevector q for $T = 0$ (thick lines) and $T = 0.1\,T_F$ (dashed lines) and several values of the dimensionless coupling $u = U_f/U_c(T) - 1 = 0.01$ (bottom pair of curves), $0.03, 0.05, \ldots, 0.13$ (top pair of curves). The insets show the dynamics phase diagram as a function of final interaction strength $U_f/U_c(0)$ and reduced temperature T/T_F. "PM" corresponds to the case where all collective are damped, while "FM" corresponds to the existence of an unstable collective mode. (b) and (d): The most unstable wavevector q_{max} and the corresponding growth rate Δ_{max} vs. the dimensionless coupling u for $T = 0$ (solid lines, both 2D and 3D), $T = 0.2\,T_F$ (dotted lines, 3D), $T = 0.1\,T_F$ (dotted lines, 2D). The dashed lines in (b) are the approximate analytical solutions.

where $c_\sigma^\dagger (c_\sigma)$ are the Fermion creation (annihilation) operators with spin σ, $\xi_{\mathbf{k}\sigma} = k^2/2m - \mu_\sigma$, m is the mass of the Fermions, μ_σ are the chemical potentials, and $U(t)$ is the time dependent coupling. $U > 0$ corresponds to the repulsive case (Stoner instability), while $U < 0$ corresponds to the attractive case (BCS pairing instability). We focus on the instantaneous quench limit, in which the coupling U changes from a negligible initial value U_i to a final value U_f at time $t = 0$. U_f is chosen to lie beyond the critical interaction strength $U_c(T)$ for the transition in question. The instantaneous quench approximation is valid if the time of ramp is much shorter than the growth rate of the instability (will be discussed later). In rapid quenches the distribution of fluctuations present in the system does not change during the quench, and is given by the equilibrium distribution at the initial value of interaction U_i. We are interested in the dynamics of this initial distribution after the quench. This dynamics is dominated by unstable collective modes which grow exponentially in time and lead to formation of textures. The equation of motion for the collective coordinate $\hat{\Phi}_{\mathbf{q}}$ is given by:

$$i\partial_t \hat{\Phi}_{\mathbf{q}}(t) = [\hat{\Phi}_{\mathbf{q}}(t), H], \qquad (2)$$

where $\hat{\Phi}_{\mathbf{q}} = S_{\mathbf{q}}^z = \frac{1}{2}\sum_{\mathbf{k}\sigma} \sigma c_{\mathbf{k+q},\sigma}^\dagger c_{\mathbf{k},\sigma}$ for the Stoner instability, while for the pairing instability, $\hat{\Phi}_{\mathbf{q}}(t) = \sum_{\mathbf{k}} c_{\mathbf{k+q},\uparrow}^\dagger c_{-\mathbf{k},\downarrow}^\dagger$. To probe the dynamics, we couple an external field $B_{\mathbf{q}}(t)$ to the collective coordinate and look at its response to this perturbation (for Stoner, the external field is just the magnetic field while for BCS, it is a fictitious pairing field). Within the framework of RPA, we obtain:

$$\Phi_{\mathbf{q}}(t) = \int \chi_{\mathbf{q}}^0(t - t')\left[U(t')\Phi_{\mathbf{q}}(t') + B_{\mathbf{q}}(t')\right], \qquad (3)$$

where $\Phi_{\mathbf{q}}(t) = \langle \hat{\Phi}_{\mathbf{q}}(t) \rangle$ and $\chi_{\mathbf{q}}^0(t - t')$ is the retarded bare susceptibility in the initial (unordered) equilibrium state. This assumes that the Fermion distribution functions do not change during the short time dynamics after a rapid quench. Eq. (3) may be interpreted as the propagation of the total field (composed of the internal mean field $U(t')\Phi_{\mathbf{q}}(t')$ and the external field $B_{\mathbf{q}}(t')$) forward in time by $\chi_{\mathbf{q}}^0(t - t')$. If the external field $B_{\mathbf{q}}(t')$, as well as $\Phi_{\mathbf{q}}(t')$ vanish for $t' \leq 0$ [10], Eq. (3) can be explicitly solved for $\Phi_{\mathbf{q}}(t)$:

$$\Phi_{\mathbf{q}}(t) = \int dt'\, \chi_{\mathbf{q}}(t - t'; U_f)B_{\mathbf{q}}(t'). \qquad (4)$$

where $\chi_{\mathbf{q}}(t - t'; U_f)$ is the inverse Fourier transform (with the integration contour shifted above all poles in the complex plane) of

$$\chi_{\mathbf{q}}(\omega; U_f) = \frac{\chi_{\mathbf{q}}^0(\omega)}{1 - U_f \chi_{\mathbf{q}}^0(\omega)}. \qquad (5)$$

This useful result relates the short time dynamics of the collective mode after a quench to an RPA-like susceptibility in which the bare response functions are evaluated in the *initial state*, but with a coupling corresponding to the *final state*. When $\chi_{\mathbf{q}}(\omega_{\mathbf{q}}; U_f)$ has poles at $\omega_{\mathbf{q}} = \Omega_{\mathbf{q}} + i\Delta_{\mathbf{q}}$ in the upper half of the complex plane, then fluctuations that occur after the quench will grow exponentially in time. In the next sections, we make these ideas explicit by studying the specific cases of the Stoner and the BCS instability.

One of the common concerns about the existence of the Stoner instability in equilibrium systems is the so called Kanamori argument [11], which says that the effective U which enters the Stoner criterion gets reduced by screening and can never exceed the Fermi energy ϵ_F. Thus the Stoner criterion is never satisfied. We note that, since we are dealing with short time dynamics of the system after a rapid quench, screening correlations do not have time to develop. So, the U_f that enters Eq.(5) is the bare U_f [12] and we always get unstable modes beyond a critical value of U.

Stoner instability– For a quench of the interaction across the Stoner instability, the magnetization propagator is given by Eq. (5), with

$$\chi_{\mathbf{q}}^0(\omega) = \int \frac{d^d\mathbf{k}}{(2\pi)^d}\frac{n^F(\xi_{\mathbf{k+q}}) - n^F(\xi_{\mathbf{k}})}{\omega - (\xi_{\mathbf{k+q}} - \xi_{\mathbf{k}}) + i0^+}, \qquad (6)$$

where $\chi^0_{\mathbf{q}}(\omega)$ is the bare spin susceptibility per spin of a free Fermi gas, and n^F is the Fermi distribution function. The poles of the corresponding propagator are then found from:

$$1 - U_f \chi^0_{\mathbf{q}}(\Omega_{\mathbf{q}} + i\Delta_{\mathbf{q}}) = 0. \tag{7}$$

A line of complex poles with a positive imaginary part $\Delta_{\mathbf{q}}$, appears when U_f exceeds $U_c(T)$ which corresponds to the Stoner instability (see insets of Fig. 1a and c). $\Delta_{\mathbf{q}}$ grows linearly for small q, reaches a maximum value, $\Delta_{\max}$ at a wave-vector $q_{\max}$, and decreases to zero at q_{cut}. Modes with $q > q_{\mathrm{cut}}$ are stable.

We begin by considering the 3D case. At $T = 0$, the integrals in Eq. (6) may be evaluated explicitly, yielding the familiar Linhardt function, analytically continued to the upper half-plane. We obtain the approximate expression for $\Delta_{\mathbf{q}}$ at $T = 0$: $\Delta^{3D}_{\mathbf{q}} = (2k_F/\pi m)uq - (1/6\pi m k_F)q^3 + \mathcal{O}(q^5)$. Fig. 1a shows $\Delta_{\mathbf{q}}$ as a function of q, for $T = 0$ and $T = 0.1\,T_F$ and several different values of $u = U_f/U_c(T) - 1$. In all cases $\Delta_{\mathbf{q}=0} = 0$ as required by the conservation of total magnetization. The values of $\Delta_{\max}$ and $q_{\max}$ are plotted as a function of u in Fig. 1b. The analytic expression for $\Delta_{\mathbf{q}}$ gives $q^{3D}_{\max} \simeq 2k_F u^{1/2}$ and $\Delta^{3D}_{\max} \simeq (16/3\pi)\epsilon_F u^{3/2}$. These approximate locations of $q_{\max}$ and $\Delta_{\max}$ appear in Fig. 1b with dashed lines, and show a good agreement with the exact numerical solution of Eq. (7) at $T = 0$. The scaling laws correspond to the critical exponents obtained for the equilibrium paramagnetic-ferromagnetic transition with $\nu = 1/2$ and $z = 3$ [13]. The temperature dependence of the above quantities have also been studied numerically and are plotted in Fig. 1a and 1b as dotted lines. We note that the scaling laws remain unchanged at finite temperatures.

Next, we consider the same instability in 2D, which is the lower critical dimension. In 2D, there is a quantum phase transition to the ferromagnetic state at $T = 0$, but there is no thermodynamic phase transition at finite temperatures. We find, however, that even at nonzero temperatures, there still is a critical interaction strength, $U_c(T)$, such that for $U_f > U_c(T)$, there are exponentially growing collective modes in the short time dynamics (see the inset of Fig 1c). At $T = 0$, Eqs. (6) and (7) yield $\Delta^{2D}_{\mathbf{q}} = \epsilon_F q[u/(1+u)]\sqrt{3 - q^2 + 2u + 1/(2u+1)}$, from which we get $\Delta^{2D}_{\max} = 2u\epsilon_F/(2u+1) \simeq 2\epsilon_F u$ and $q^{2D}_{\max} = k_F\sqrt{u + [3 + 1/(2u+1)]/2} \simeq \sqrt{2}k_F$. In Fig. 1c and 1d we plot the same quantities as in Fig. 1a and 1b, but for the 2D case. The major difference in 2D is that, at finite temperatures, $\mathbf{q}^{2D}_{\max}$ starts at $\mathbf{q} = 0$ for $u = 0$ and rapidly grows to $\sqrt{2}k_F$ as one quenches deeper into the unstable side. From a low temperature expansion, we find that at $T \neq 0$, $\mathbf{q}^{2D}_{\max} \sim u^{1/2}(T)^{1/2}\exp(\epsilon_F/2T)$ while $\Delta_{\max} \sim u^{3/2}(T\epsilon_F)^{1/2}\exp(\epsilon_F/2T)$ for small u. These scaling solutions go over to the $T = 0$ scaling forms when $u \sim (k_F/T)\exp(-\epsilon_F/T)$, which is an exponentially small region at small T.

Pairing instability– In this section we consider the instability of a 3D Fermi gas with attractive interactions at $T = 0$. The case with no spin imbalance has been studied in the liter-

ature before [14]. Here, we study the general case with spin imbalance. We start by noting that the bare BCS susceptibility has a ultraviolet divergence which is regularized by expressing the microscopic interaction strength, U_f, in terms of the s-wave scattering length [15]. Following this regularization procedure, we obtain an expression for the poles of the propagator of the pairing fluctuations [the equivalent of Eq. (7)]:

$$\frac{m}{4\pi a_s} = \int \frac{d^d\mathbf{k}}{(2\pi)^d}\left(\frac{1 - n^F(\xi_{\mathbf{k},\uparrow}) - n^F(\xi_{-\mathbf{k}+\mathbf{q},\downarrow})}{\omega_{\mathbf{q}} - \xi_{\mathbf{k}\uparrow} - \xi_{-\mathbf{k}+\mathbf{q}\downarrow} + i0^+} + \frac{m}{\mathbf{k}^2}\right), \tag{8}$$

where $\omega_{\mathbf{q}} = \Omega_{\mathbf{q}} + i\Delta_{\mathbf{q}}$, and $a_s < 0$ is the final s-wave scattering length. In Fig. 2a, we plot $\Delta_{\mathbf{q}}$ as a function of q, for several values of spin imbalance $\delta = (n_\uparrow - n_\downarrow)/(n_\uparrow + n_\downarrow)$ and a final s-wave scattering length $k_F a_s = -0.4$. For the spin-balanced case we recover the approximate solution $\Delta_{\mathbf{q}} \approx \Delta_0 - 2q^2/3k_F^2\Delta_0 - \mathcal{O}(q^4)$, where $\Delta_0 = 8\epsilon_F\exp(\pi/2a_s - 2)$, from which we infer $q_{\mathrm{cut}} = (\sqrt{3/2})\Delta_0 k_F$. We note that $\Delta_0 = \Delta_{\mathrm{BCS}}$, i.e. the growth rate of the BCS type pairings is proportional to the BCS gap at equilibrium [14]. Thus, for the spin balanced case the growth rate decreases monotonically with $\mathbf{q}$ and the strongest instability is towards pairing with zero center of mass momentum. The same picture holds at small but finite population imbalances. However, as δ crosses a critical value, the maximum of the growth rate continuously shifts to a nonzero q. Thus, for large enough δ, the short time dynamics is dominated by finite-momentum pairings. This is illustrated in Fig. 2b where we plot the wave-vector of the most unstable state, $q_{\max}$, as a function of spin imbalance δ for several values of $k_F a_s$. As the imbalance is increased further, the zero momentum pairing instability disappears completely (corresponding to Clogston-Chandrasekhar limit [16]). Finally, all pairing instabilities disappear at larger population imbalances, which corresponds to the sudden end of the curves in Fig. 2b at large δ.

In the inset of Fig. 2, we have plotted the phase diagram of the system as determined by the nature of the dominant unstable mode in the coupling ($k_F a_s$) and the spin imbalance, (δ) plane. Note that FFLO is used in a loose sense of finite momentum pairing while BCS corresponds to zero momentum pairing. This diagram resembles the mean-field *equilibrium* phase diagram [9], with the significant difference being a larger region dominated by finite-momentum pairings. We finally note that instead of directly probing the pairing order parameter, one can look for spin correlations associated with finite wave-vector pairings through interactions in the Cooper channel, which are expected to appear for quenches with sufficiently large spin imbalances.

Comment regarding lattice– One interesting extension of our work is analysis of the timescale of formation of antiferromagnetic order in optical lattices for interaction strength which are not too large. In these cases, antiferromagnetic order relies on the BCS type instability of the nested Fermi surface [17]. Therefore, the quench dynamics is expected to have resemblances with the behavior shown in Fig. 2.

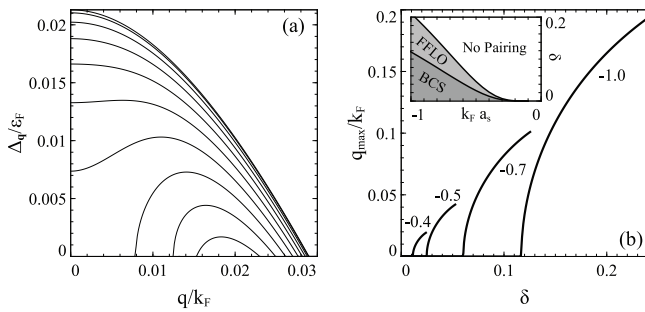*Cold atom experiments*– Finally, we would like to comment

FIG. 2: Unstable collective modes in the BCS instability in 3D. (a) Growth rate of modes, Δ_q, as a function of wavevector q for various values of the population imbalance $\delta = 0$ (top curve), 0.0025, $\ldots$, 0.0225 (bottom curve); ($k_F a_s = -0.4$). (b) The most unstable wavevector q_{max} as a function of δ for various values of the $k_F a_s$ (indicated). As δ increases, q_{max} goes through a continuous transition; the curves terminate at large δ, above which all pairing modes are stable. Inset: the phase diagram in the $k_F a_s$-δ plane, showing the character of the most unstable mode.

on the possibility of observing the described dynamics of texture growth in realistic cold atom experiments. There are two issues here: (a) the length scale corresponding to the most unstable mode and (b) the time scale associated to the growth of unstable modes. The length scale $1/q_{max}$ must be sufficiently large so that patterns can be resolved. Achieving large pattern sizes requires a quench to a final coupling which is close to the critical value. However, the growth rate Δ_{max} is small in this regime and the textures develop over a long time. Therefore, one needs to find a window of U_f, where the length scale is resolved in experiments while the timescale is short enough to prevent considerable atom losses. In recent experiments [7], the quench time was ~ 4 ms, which was followed by a hold time of upto ~ 12 ms; the imaging resolution was $\sim 10 k_F^{-1}$.

We note that the quench approximation is applicable for $\Delta_{max}[U(t)]^{-1} \sim t - t_c$, where t_c is the time at which the instability is crossed, i.e. $U(t_c) = U_c$. Since $t - t_c$ may be significantly smaller than t, the validity regime of our calculations can be large. Based on this, the quench approximation is applicable to the MIT experiment with final couplings $U_f/U_c \lesssim 1.06$. Moreover, in order to have resolvable textures in the experiment, $U_f/U_c \lesssim 1.004$, which corresponds to growth timescales of $\gtrsim 14$ ms, which is of the same order as the experimental hold times. In current experiments, the typical step in $k_F a_s$ was 0.3, thus we would expect that the smallest U_f that exceeded U_c was $U_f \sim 1.06\, U_c$, which corresponds to the expected pattern size of $\sim 2k_F^{-1}$. This is consistent with the fact that individual textures were not resolved in the current set of experiments. Our theory indicates that finer tuning of the interaction strength may in fact produce textures large enough to be resolvable, although inhomogeneous density profiles make it more difficult to observe.

[1] I. Bloch, J. Dalibard and W. Zwerger, Rev. Mod. Phys. **80**, 885 (2008)

[2] K. Sengupta, S. Powell and S. Sachdev, Phys. Rev. A. **69**, 053616 (2004); W. H. Zurek, U. Dorner and P. Zoller, Phys. Rev. Lett. **95**, 105701 (2005); M. Rigol and A. Muramatsu, Phys. Rev. Lett. **94**, 240403 (2005); A. Polkovnikov, Phys. Rev. B **72**, 161201 (R) (2005); R. W. Cherng and L. S. Levitov, Phys. Rev. A **73**, 043614 (2006); U. Schollwock and S. R. White in *Effective Models for Low Dimensional Strongly Correlated Systems*, (G. G. G. Batrouni and D. Poilblanc ed., AIP, Melville, New York, 2006); S. R. Manmana, S. Wessel, R. M. Noack and A. Muramutsu, Phys. Rev. Lett. **98**, 210405 (2007); H. Saito, Y. Kawaguchi, M. Ueda, Phys. Rev. A **75**, 013621 (2007); A. Lamacraft, Phys. Rev. Lett. **98**, 160404 (2007); R. Bistritzer and E Altman, Proc. Natl. Acad. of Sc. **104**, 9955 (2007); C. Kollath, A. M. Lauchli, E. Altman, Phys. Rev. Lett. **98**, 180601 (2007); A. Polkovnikov and V. Gritsev, Nature Phys. **4**, 477 (2008); M. Rigol, V. Dunjko, M. Olshanii, Nature **452**, 854 (2008); A. Faribault, P. Calabrese, J.-S. Caux, arXiv:0812.1928; S. Mondal, K. Sengupta, and D. Sen, Phys. Rev. B **79**, 045128 (2009); D. Dagnino, N. Barbern, M. Lewenstein, J. Dalibard, Nature Physics **5**, 431 (2009); A. Iucci and M. A. Cazalilla, arXiv:0903.1205;

[3] N. Strohmaier *et. al*, cond-mat/0905.2963

[4] H. J. Miesner *et. al*, Phys. Rev. Lett. **82**, 2228 (1999); H. Schmaljohann, Phys. Rev. Lett. **92**, 040402 (2004); L. E. Sadler et. al., Nature **443**, 312 (2006).

[5] M. Greiner, O. Mandel, T.W. Hansch, I. Bloch, Nature **419**, 51 (2002).

[6] J. L. Roberts, N. R. Claussen, S. L. Cornish, E. A. Donley, E. A. Cornell, and C. E. Wieman, Phys. Rev. Lett. **86**, 4211 (2001).

[7] G.-B. Jo *et. al*, arXiv:0907.2888.

[8] E. Stoner, Phil. Mag. **15**, 1018 (1933); Y. Zhang and S. Das Sarma, Phys. Rev. B **72** , 115317 (2005); R. A. Duine and A. H. McDonald, Phys. Rev. Lett. **95**, 230403 (2005); G. J. Conduit and B. D. Simons, Phys. Rev. A **79**, 053606 (2009).

[9] D. E. Sheehy and L. Radzihovsky, Ann. of Phys. **322**, 1790 (2007)

[10] Both of these conditions can be easily relaxed. However, the simple case already exhibits the important physical features.

[11] J. Kanamori, Prog. Theor. Phys. **30**, 275 (1963)

[12] For finite U_i, the final coupling U_f is renormalized by a screening cloud corresponding to U_i and so, for small U_i, it never reaches the Kanamori limit. One should work with the Landau quasiparticles corresponding to U_i when computing χ^0

[13] H. V. Lohneysen, A. Rosch, M. Vojta and P. Wolfle, Rev. Mod. Phys. **79**, 1015 (2007).

[14] A. A. Abrikosov, L. P. Gorkov, I. E. Dzyaloshinski, *Methods of quantum field theory in statistical physics*, (Dover Publications, New York, 1975).

[15] C. A. S. de Melo, M. Randeria, and J. R. Engelbrecht, Phys. Rev. Lett. **71**, 3202 (1993).

[16] B. S. Chandrasekhar, App. Phys. Lett. **1**, 7 (1962); A. M. Clogston, Phys. Rev. Lett. **9**, 266 (1962).

[17] V. J. Emery, Phys. Rev. B **14**, 2989 (1976).